Atmospheric
Chemistry
and Physics

*Supplement of*

# Geochemistry of PM$_{10}$ over Europe during the EMEP intensive measurement periods in summer 2012 and winter 2013

**Andrés Alastuey et al.**

*Correspondence to:* Andrés Alastuey (andres.alastuey@idaea.csic.es)

**Table S1: Average minimum detection limit (MDL) for the elements measured by PIXE.**

| | MDL | | | | |
| --- | --- | --- | --- | --- | --- |
| | ng/cm$^2$ | ng/m$^3$ | | ng/cm$^2$ | ng/m$^3$ |
| Na | 24.8 | 5.5 | Ti | 4.8 | 1.1 |
| Mg | 18.9 | 4.2 | V | 3.4 | 0.7 |
| Al | 12.7 | 2.8 | Cr | 2.1 | 0.5 |
| Si | 10.2 | 2.3 | Mn | 1.5 | 0.3 |
| P | 9.3 | 2.0 | Ni | 0.6 | 0.1 |
| S | 9.9 | 2.2 | Cu | 0.6 | 0.1 |
| Cl | 11.1 | 2.5 | Zn | 0.6 | 0.1 |
| K | 11.5 | 2.5 | As | 0.8 | 0.2 |
| Ca | 9.2 | 2.0 | Se | 0.9 | 0.2 |
| Fe | 1.1 | 0.2 | Br | 1.2 | 0.3 |
| | | | Rb | 1.9 | 0.4 |
| | | | Sr | 2.5 | 0.5 |
| | | | Zr | 4.0 | 0.9 |
| | | | Mo | 7.4 | 1.6 |
| | | | Ba | 12.8 | 2.8 |
| | | | Pb | 1.7 | 0.4 |

**Table S2. Slope and R2 determination coefficients for concentrations determined by PIXE and ICPs (PIXE = a * ICPs) at ES1778. n= number of data pairs available for the correlation.**

| | ICPs ES1778 | | | | | |
| --- | --- | --- | --- | --- | --- | --- |
| | | y=ax | | | y=ax + b | |
| | n | slope | R$^2$ | slope | constant | R$^2$ |
| Al | 38 | 1.02 | 0.99 | | | |
| Fe | 38 | 1.04 | 0.99 | | | |
| K | 38 | 1.03 | 0.97 | | | |
| Mg | 38 | 1.26 | 0.97 | | | |
| Ca | 38 | 1.05 | 0.95 | | | |
| S | 38 | 1.01 | 0.93 | | | |
| Na | 38 | 1.13 | 0.91 | | | |
| Si | -- | -- | -- | -- | -- | -- |
| Ti | 37 | 1.22 | 0.98 | | | |
| Mn | 34 | 1.03 | 0.98 | | | |
| Zn | 38 | 1.04 | 0.81 | 0.90 | 2.18 | 0.84 |
| Cu | 37 | 1.11 | 0.71 | 0.89 | 0.75 | 0.76 |
| V | 26 | 1.29 | 0.49 | 0.93 | 2.19 | 0.63 |
| Pb | 11 | 0.94 | 0.40 | 0.63 | 1.37 | 0.60 |
| Cr | 21 | 1.64 | -0.72 | 0.81 | 2.60 | 0.69 |
| Sr | 12 | 0.77 | -2.01 | 0.30 | 3.39 | 0.65 |
| Ni | 35 | 1.14 | -0.44 | 0.48 | 1.58 | 0.19 |
| Cl | 38 | 0.62 | 0.31 | 0.69 | 2.93 | 0.32 |

**Table S3. Mean concentrations of PM10, major (µg m$^{-3}$) and trace elements (ng m$^{-3}$) during the summer 2012 IMP.**

| Summer | AM01 | CH02 | DE44 | GR02 | IT04 | MD13 | SE12 | SK06 | GB48 | IT01 | ES778 | FR30 | HU02 | ESCLl | IE31 | FR22 | FR09 | ES22 |
|---|---|---|---|---|---|---|---|---|---|---|---|---|---|---|---|---|---|---|
| N | 32 | 40 | 37 | 39 | 37 | 44 | 26 | 32 | 32 | 39 | 41 | 22 | 39 | 17 | 31 | 7 | 7 | 28 |
| µg m$^{-3}$ | | | | | | | | | | | | | | | | | | |
| PM$_{10}$ | 14.0 | 12.3 | 20.0 | 25.0 | 14.8 | 26.2 | 7.7 | 15.2 | 4.5 | 31.1 | 27.50 | 2.9 | 15.3 | 18.1 | 12.9 | -- | 13.6 | 21.0 |
| Na | 0.06 | 0.11 | 0.14 | 1.30 | 0.20 | 0.11 | 0.36 | 0.08 | 0.22 | 0.80 | 0.70 | 0.04 | 0.02 | 0.93 | 0.77 | 0.27 | 0.37 | 0.33 |
| Mg | 0.23 | 0.05 | 0.05 | 0.28 | 0.09 | 0.21 | 0.06 | 0.07 | 0.04 | 0.23 | 0.23 | 0.02 | 0.09 | 0.25 | 0.12 | 0.13 | 0.10 | 0.18 |
| Al | 0.50 | 0.15 | 0.13 | 0.39 | 0.23 | 0.87 | 0.04 | 0.28 | 0.03 | 0.62 | 0.61 | 0.07 | 0.37 | 0.31 | 0.04 | 0.45 | 0.25 | 0.73 |
| Si | 1.32 | 0.37 | 0.30 | 0.97 | 0.59 | 2.46 | 0.10 | 0.67 | 0.08 | 1.34 | 1.29 | 0.16 | -- | 0.72 | 0.04 | 0.95 | 0.51 | -- |
| Ca | 0.69 | 0.18 | 0.08 | 0.44 | 0.16 | 0.77 | 0.04 | 0.14 | 0.03 | 1.42 | 0.52 | 0.03 | 0.35 | 0.64 | 0.04 | 0.31 | 0.15 | 0.68 |
| Fe | 0.29 | 0.13 | 0.11 | 0.30 | 0.26 | 0.62 | 0.04 | 0.19 | 0.03 | 0.48 | 0.36 | 0.03 | 0.23 | 0.22 | 0.01 | 0.25 | 0.15 | 0.40 |
| S | 0.76 | 0.36 | 0.66 | 1.97 | 0.85 | 1.12 | 0.53 | 0.88 | 0.37 | 1.15 | 0.92 | 0.17 | 0.66 | 0.72 | 0.39 | 0.60 | 0.58 | 0.59 |
| Cl | 0.02 | 0.03 | 0.04 | 1.05 | 0.02 | 0.02 | 0.08 | 0.01 | 0.15 | 0.39 | 0.17 | <0.1 | - | 0.80 | 1.12 | 0.10 | 0.16 | 0.09 |
| K | 0.19 | 0.12 | 0.12 | 0.25 | 0.14 | 0.44 | 0.06 | 0.17 | 0.04 | 0.35 | 0.23 | 0.03 | 0.09 | 0.17 | 0.04 | 0.18 | 0.11 | 0.17 |
| ng m$^{-3}$ | | | | | | | | | | | | | | | | | | |
| P | 3.8 | 23.4 | 31.0 | 3.2 | 7.5 | 14.1 | 7.6 | 21.5 | 5.8 | 9.6 | 11.1 | 0.8 | <0.5 | 11.8 | 4.7 | 26.9 | 13.3 | 17.9 |
| Ti | 31.7 | 9.9 | 8.3 | 27.2 | 14.6 | 56.3 | 3.0 | 18.9 | 2.9 | 36.3 | 42.8 | 4.8 | 22.8 | 21.5 | 3.0 | 29.0 | 15.2 | 48.8 |
| V | 0.5 | 0.7 | 1.1 | 6.2 | 1.7 | 1.9 | 1.0 | 1.0 | 0.9 | 4.8 | 4.8 | 0.2 | 1.0 | 3.9 | 1.4 | 2.2 | 1.7 | 2.8 |
| Cr | 1.3 | 1.0 | 1.6 | 1.1 | 1.1 | 2.2 | 0.3 | 4.4 | 0.6 | 2.6 | 2.8 | 0.2 | 1.8 | 2.3 | 1.1 | 1.3 | 1.1 | 1.3 |
| Mn | 9.0 | 2.8 | 3.0 | 6.8 | 4.2 | 16.9 | 1.2 | 4.6 | 0.9 | 9.8 | 6.9 | 0.9 | 7.0 | 4.2 | 0.8 | 5.5 | 3.6 | 9.9 |
| Ni | 1.1 | 0.5 | 0.8 | 2.5 | 1.3 | 1.1 | 0.9 | 2.1 | 0.6 | 2.2 | 2.1 | 0.2 | 3.3 | 1.7 | 0.6 | 0.6 | 0.5 | 1.1 |
| Cu | 1.3 | 2.8 | 2.7 | 2.0 | 8.3 | 2.5 | 0.8 | 2.4 | 0.8 | 11.1 | 3.4 | 0.5 | 4.0 | 2.9 | 0.7 | 2.4 | 1.8 | 2.0 |
| Zn | 12.4 | 7.5 | 14.3 | 21.9 | 14.4 | 18.0 | 4.5 | 19.7 | 8.2 | 18.9 | 14.5 | 5.4 | 7.3 | 7.4 | 12.0 | 17.2 | 20.1 | 6.4 |
| As | 1.6 | 0.2 | 0.6 | 0.6 | 0.2 | 0.6 | 0.3 | 0.7 | 0.3 | 0.1 | 0.8 | 0.1 | 0.5 | 0.7 | 0.3 | 0.6 | 0.5 | 0.2 |
| Se | 0.6 | 0.2 | 0.6 | 0.6 | 0.4 | 1.1 | 0.2 | 0.5 | 0.3 | 0.5 | 1.1 | 0.0 | 0.3 | 0.9 | 0.4 | 0.6 | 0.8 | 0.3 |
| Br | 2.4 | 1.4 | 2.3 | 8.4 | 2.8 | 3.3 | 1.9 | 1.8 | 1.3 | 5.0 | 3.4 | 0.5 | <0.5 | 4.9 | 3.3 | 2.2 | 1.9 | <0.5 |
| Rb | 1.7 | 0.8 | 0.6 | 1.3 | 0.9 | 3.0 | 0.2 | 0.9 | 0.4 | 4.1 | 2.7 | - | 0.4 | 2.1 | 0.8 | 1.2 | 1.1 | 0.8 |
| Sr | 2.3 | 0.6 | 0.9 | 2.8 | 4.2 | 3.5 | 0.4 | 1.1 | 0.5 | 6.0 | 3.3 | 0.2 | 1.1 | 3.5 | 1.2 | 1.7 | 1.3 | 3.7 |
| Zr | 1.1 | 0.7 | 1.2 | 1.4 | 1.1 | 2.0 | 0.5 | 1.2 | 0.8 | 2.3 | 5.1 | 0.1 | 8.8 | 5.0 | 1.8 | 2.2 | 2.1 | 4.9 |
| Mo | 2.3 | 0.9 | 2.1 | 2.1 | 1.5 | 2.3 | 0.9 | 2.1 | 1.5 | 0.2 | 8.7 | <0.2 | 7.0 | 7.8 | 3.2 | 4.0 | 3.7 | <0.2 |
| Ba | 3.1 | 1.8 | 3.5 | 4.4 | 16.0 | 6.5 | 1.6 | 4.1 | 2.4 | 7.4 | 0.0 | <0.2 | 3.8 | 8.1 | 5.1 | 9.2 | 7.3 | 5.0 |
| Pb | 7.5 | 1.2 | 2.3 | 15.2 | 3.8 | 5.8 | 1.2 | 2.4 | 0.9 | 4.1 | 2.1 | 0.2 | 2.7 | 1.9 | 0.8 | 2.4 | 2.5 | 1.6 |

**Table S4. Mean concentrations of PM10, major (µg m$^{-3}$) and trace elements (ng m$^{-3}$) during the winter 2013 IMP.**

| Winter | CH02 | DE44 | GR02 | IT04 | MD13 | SE12 | SK06 | GB48 | IT01 | ES1778 | FR30 | HU02 | IE31 | FR22 | FR09 | FR20 | GB36 | ES22 |
|---|---|---|---|---|---|---|---|---|---|---|---|---|---|---|---|---|---|---|
| N | 29 | 28 | 30 | 29 | 29 | 29 | 29 | 20 | 29 | 31 | 12 | 26 | 14 | 9 | 6 | 8 | 26 | 22 |
| **µg m$^{-3}$** | | | | | | | | | | | | | | | | | | |
| PM$_{10}$ | 16.1 | 28.1 | 39.7 | 37.4 | 28.6 | 6.8 | 17.7 | 7.5 | 23.6 | 9.2 | -- | 20.3 | 35.7 | 20.5 | 25.4 | -- | 17.9 | 3.4 |
| Na | 0.18 | 0.31 | 1.51 | 0.21 | 0.13 | 0.34 | 0.10 | 0.91 | 0.57 | 0.20 | 0.01 | 0.49 | 6.10 | 0.38 | 0.28 | 0.40 | 1.00 | 0.06 |
| Mg | 0.03 | 0.06 | 0.76 | 0.05 | 0.05 | 0.06 | 0.02 | 0.15 | 0.13 | 0.05 | 0.01 | 0.03 | 1.00 | 0.07 | 0.06 | 0.07 | 0.17 | 0.01 |
| Al | 0.02 | 0.07 | 1.09 | 0.09 | 0.10 | 0.01 | 0.04 | 0.02 | 0.09 | 0.08 | 0.02 | 0.12 | 0.12 | 0.02 | 0.03 | 0.04 | 0.02 | 0.02 |
| Si | 0.08 | 0.14 | 2.55 | 0.23 | 0.25 | 0.04 | 0.09 | 0.04 | 0.20 | 0.17 | 0.04 | -- | 0.04 | 0.06 | 0.07 | 0.12 | 0.06 | -- |
| Ca | 0.08 | 0.07 | 2.37 | 0.16 | 0.09 | 0.03 | 0.07 | 0.04 | 0.25 | 0.09 | 0.01 | 0.07 | 0.25 | 0.06 | 0.07 | 0.11 | 0.07 | 0.05 |
| Fe | 0.08 | 0.07 | 0.67 | 0.42 | 0.12 | 0.03 | 0.05 | 0.02 | 0.15 | 0.05 | 0.01 | 0.02 | 0.01 | 0.07 | 0.10 | 0.20 | 0.08 | 0.01 |
| S | 0.47 | 1.18 | 0.58 | 0.66 | 1.27 | 0.46 | 1.23 | 0.28 | 0.41 | 0.15 | 0.05 | 0.81 | 0.55 | 0.99 | 1.24 | 0.89 | 0.67 | 0.05 |
| Cl | 0.21 | 0.31 | 2.18 | 0.40 | 0.18 | 0.19 | 0.01 | 1.06 | 0.54 | 0.08 | <0.1 | - | 11.2 | 0.32 | 0.37 | 0.53 | 1.14 | 0.10 |
| K | 0.20 | 0.15 | 0.44 | 0.57 | 0.32 | 0.08 | 0.24 | 0.05 | 0.39 | 0.08 | 0.01 | 0.22 | 0.25 | 0.14 | 0.12 | 0.17 | 0.10 | 0.03 |
| **ng m$^{-3}$** | | | | | | | | | | | | | | | | | | |
| P | 7.3 | 3.2 | 5.8 | 4.2 | 1.5 | 1.1 | 2.8 | 1.7 | 3.3 | 2.8 | 1.2 | <0.5 | 6.2 | 2.2 | 2.5 | 2.4 | 2.1 | <0.5 |
| Ti | 2.1 | 4.8 | 69.6 | 7.1 | 6.7 | 1.0 | 2.7 | 1.4 | 5.7 | 4.7 | 0.6 | 2.8 | 2.8 | 1.7 | 3.2 | 3.9 | 2.0 | 3.6 |
| V | 0.4 | 1.1 | 3.4 | 0.9 | 1.0 | 0.5 | 1.0 | 0.7 | 1.0 | 1.0 | 0.5 | 0.4 | 1.9 | 0.7 | 1.2 | 1.2 | 1.0 | 0.1 |
| Cr | 0.9 | 0.8 | 1.7 | 2.7 | 0.5 | 0.3 | 1.2 | 0.4 | 3.7 | 0.7 | 0.3 | 1.3 | 1.7 | 1.1 | 2.0 | 1.8 | 0.8 | 1.2 |
| Mn | 2.3 | 2.7 | 10.0 | 6.6 | 3.5 | 1.5 | 2.2 | 0.5 | 3.3 | 2.3 | 0.2 | 1.1 | 1.0 | 3.6 | 5.2 | 4.6 | 1.7 | 0.8 |
| Ni | 0.3 | 0.7 | 1.2 | 1.9 | 0.7 | 0.5 | 0.8 | 0.4 | 2.1 | 0.4 | 0.2 | 0.8 | 0.8 | 0.7 | 1.0 | 1.1 | 0.7 | 0.1 |
| Cu | 3.6 | 3.3 | 1.4 | 15.9 | 2.3 | 0.9 | 2.2 | 0.9 | 5.7 | 2.3 | 0.5 | 0.1 | 1.0 | 2.3 | 3.2 | 9.4 | 3.4 | 0.3 |
| Zn | 17.9 | 35.7 | 19.0 | 36.0 | 24.5 | 15.0 | 27.7 | 9.9 | 18.4 | 14.4 | 5.1 | 11.4 | 16.4 | 37.5 | 59.1 | 40.9 | 22.9 | 3.0 |
| As | 0.3 | 1.3 | 0.6 | 0.7 | 1.2 | 0.4 | 0.8 | 0.4 | 0.3 | 0.3 | 0.1 | 1.2 | 0.5 | 0.4 | 0.7 | 0.6 | 0.9 | 0.1 |
| Se | 0.3 | 0.6 | 0.6 | 0.7 | 0.6 | 0.2 | 0.4 | 0.2 | 0.3 | 0.2 | 0.1 | 0.3 | 0.7 | 1.0 | 1.1 | 0.9 | 0.5 | <0.2 |
| Br | 2.0 | 5.2 | 8.7 | 5.0 | 5.2 | 2.1 | 3.3 | 2.8 | 5.4 | 1.6 | 0.2 | <0.2 | 28.6 | 3.3 | 5.1 | 6.1 | 5.6 | <0.2 |
| Rb | 0.8 | 0.6 | 4.2 | 3.1 | 1.3 | 0.3 | 0.7 | 0.4 | 2.8 | 0.5 | 0.2 | 0.5 | 1.5 | 0.7 | 0.6 | 1.5 | 0.4 | <0.2 |
| Sr | 0.4 | 0.8 | 8.5 | 16.3 | 0.8 | 0.4 | 0.7 | 0.8 | 1.6 | 0.7 | 0.3 | 0.4 | 5.6 | 0.7 | 0.7 | 0.9 | 1.0 | 0.2 |
| Zr | 0.6 | 1.0 | 3.5 | 1.5 | 0.7 | 0.5 | 1.0 | 0.8 | 1.1 | 0.9 | 0.5 | 11.0 | 2.9 | 1.1 | 1.1 | 1.6 | 0.9 | 0.4 |
| Mo | 0.9 | 1.7 | 3.1 | 2.1 | 1.0 | 0.9 | 1.8 | 1.4 | 1.1 | 1.7 | 1.0 | 3.0 | 5.2 | 1.7 | 1.9 | 1.7 | 1.5 | <0.2 |
| Ba | 2.0 | 3.8 | 14.8 | 31.8 | 2.3 | 1.5 | 3.9 | 2.3 | 3.4 | 3.6 | 1.5 | 0.8 | 7.8 | 3.7 | 3.3 | 5.1 | 3.5 | 0.9 |
| Pb | 3.7 | 9.9 | 15.0 | 10.7 | 9.6 | 1.5 | 6.9 | 0.9 | 5.3 | 1.4 | 0.5 | 6.0 | 1.1 | 7.2 | 6.9 | 12.0 | 6.5 | 0.2 |

**Figure**
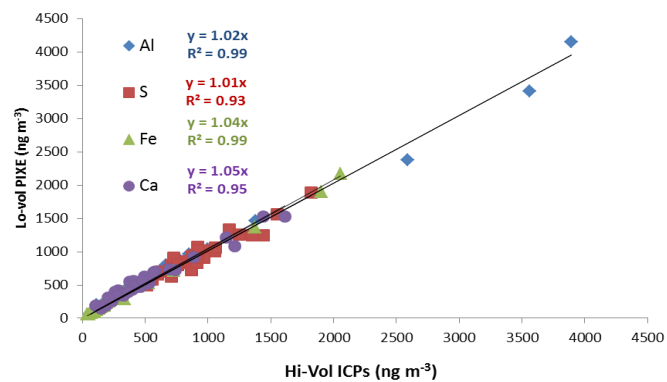


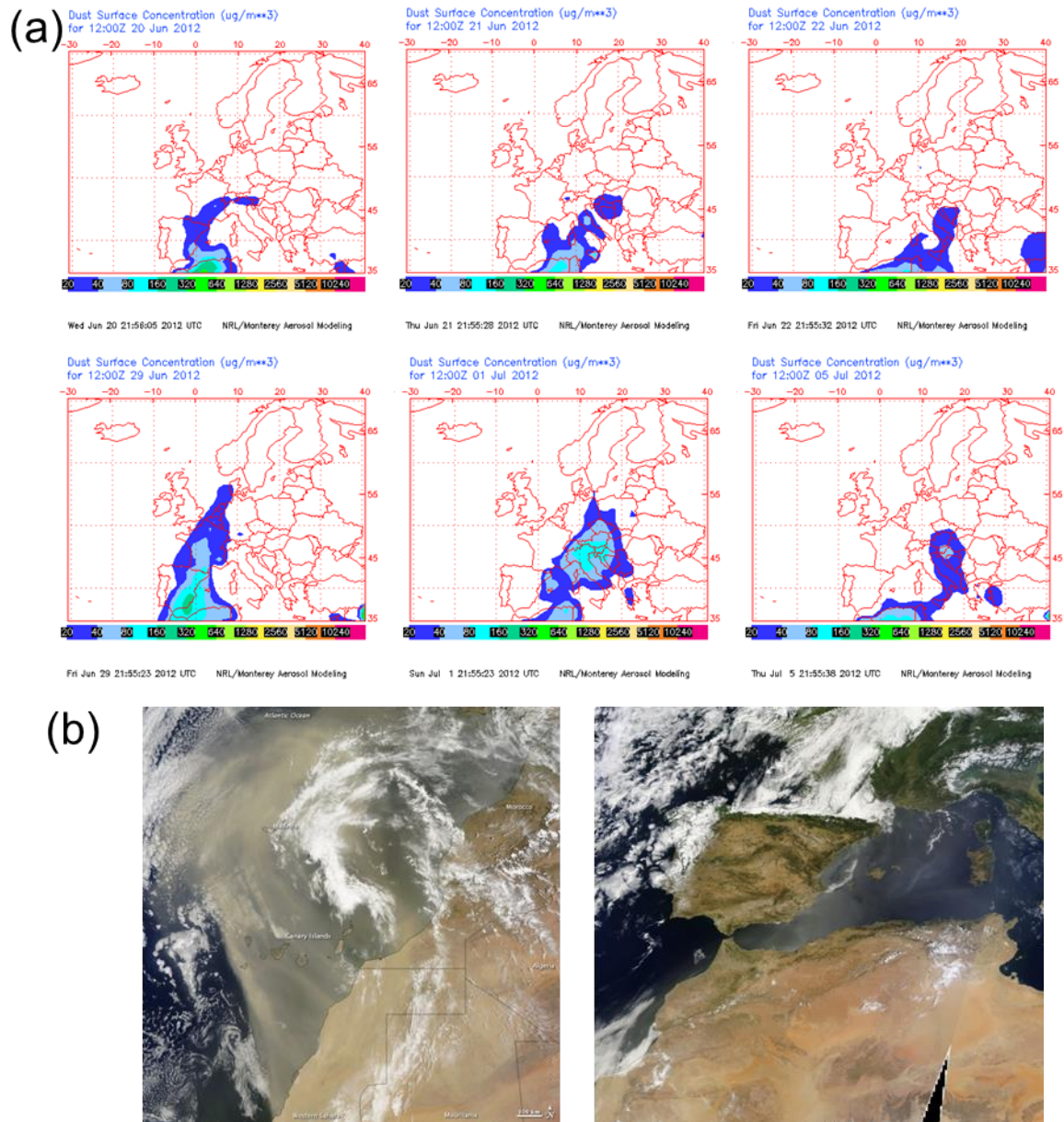**Figure S1: Correlation between concentrations of major elements determined by PIXE and ICPs at ES1778.**

**Figure S2:** Two major dust episodes were observed in June/July 2012. For both cases, the dust outbreak was transported eastwards. As shown by: (a) dust surface concentration maps by NAAPS Navy Aerosol Analysis Prediction System from the Marine Meteorology Division of the Naval research Laboratory, USA (NRL) for June 20, 21, 22, 29 and July 01 and 05; (b) NASA Terra – MODIS, images courtesy MODIS Rapid Response Team, Goddard Space Flight Centre. Left: 2012/06/25. Right: 2012/06/30.
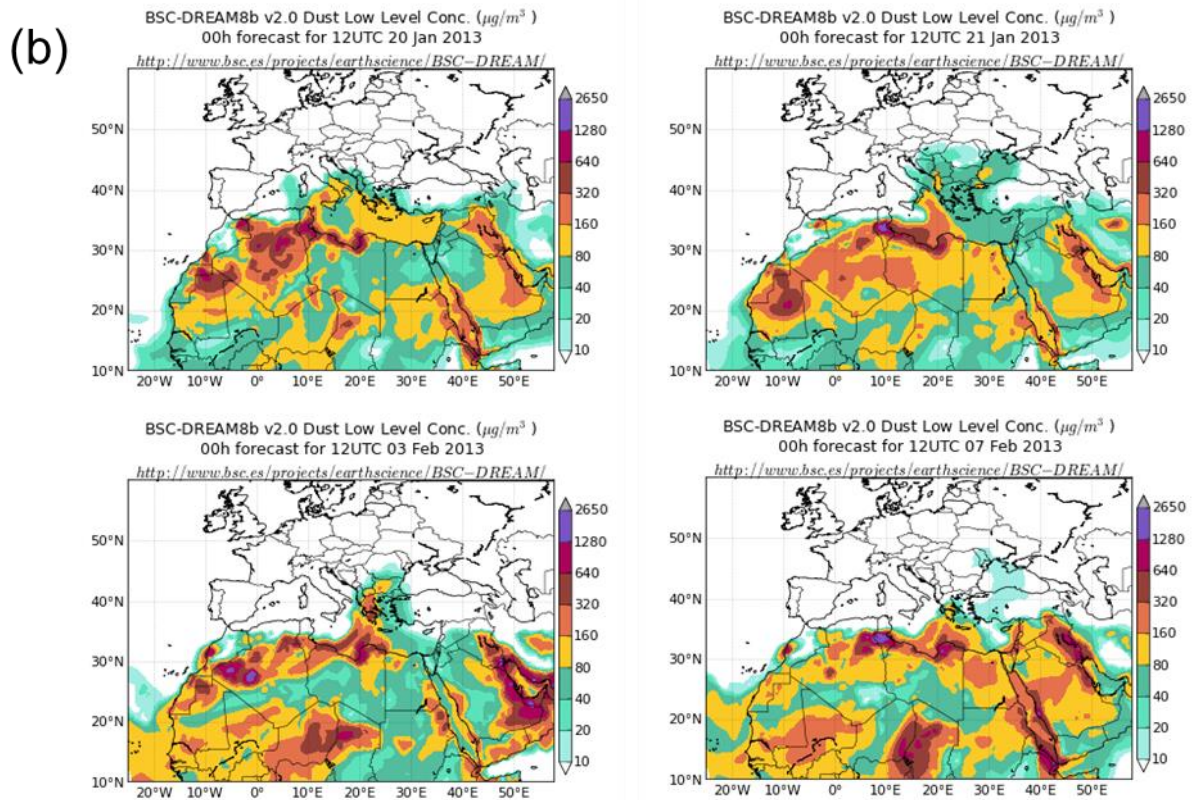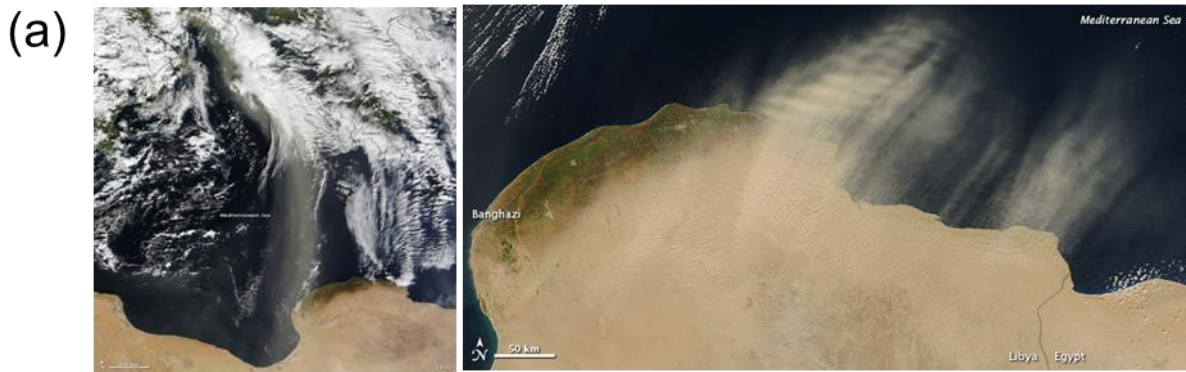
**Figure S3: During the winter IMP, the eastern region was affected by short but intense pulses of dust. (a) Satellite images courtesy MODIS Rapid Response Team, Goddard Space Flight Center. Left: Terra – MODIS, 2013/01/21. Right: Aqua – MODIS Multiple dust plumes 2013/02/07 moving off the coast of Libya toward the northeast. (b) Maps of dust surface concentration from the BSC-DREAM8b (Dust REgional Atmospheric Model) model, operated by the Barcelona Supercomputing Center (BSC) for January 20 and 21 and February 03 and 07.**
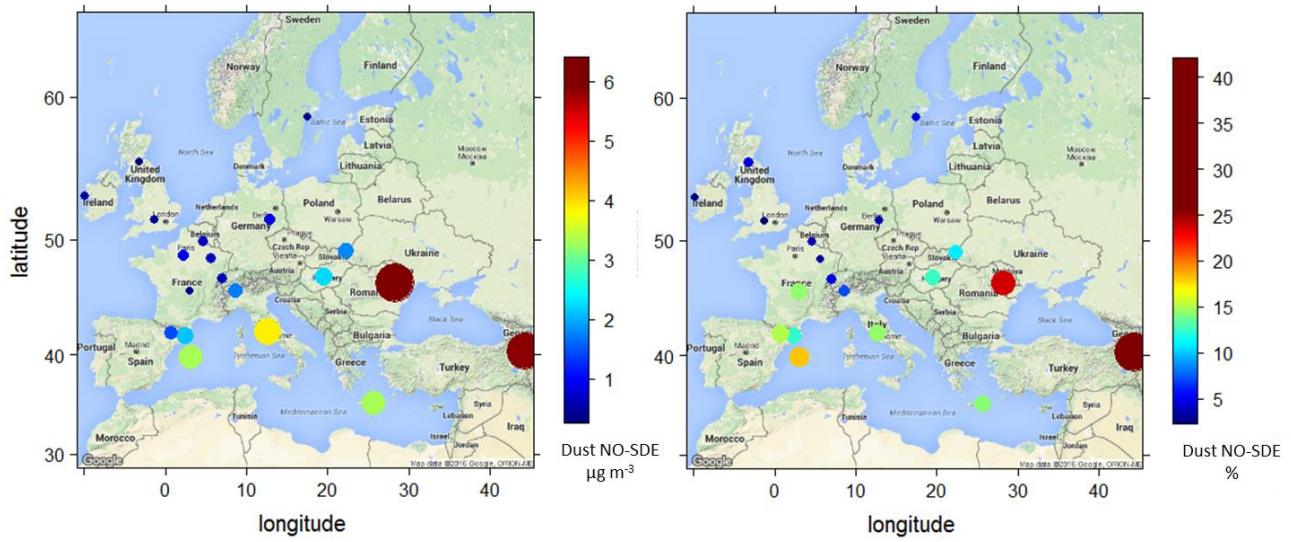
**Figure S4:** Spatial distribution of the average mineral dust concentration (μg m^-3) and its relative contribution (%) to $PM_{10}$ obtained at each site in the summer 2012 and the winter 2013 IMPs during the Non-Saharan dust events (NO-SDE). The diameter of the circles is proportional to the concentrations and percentages.
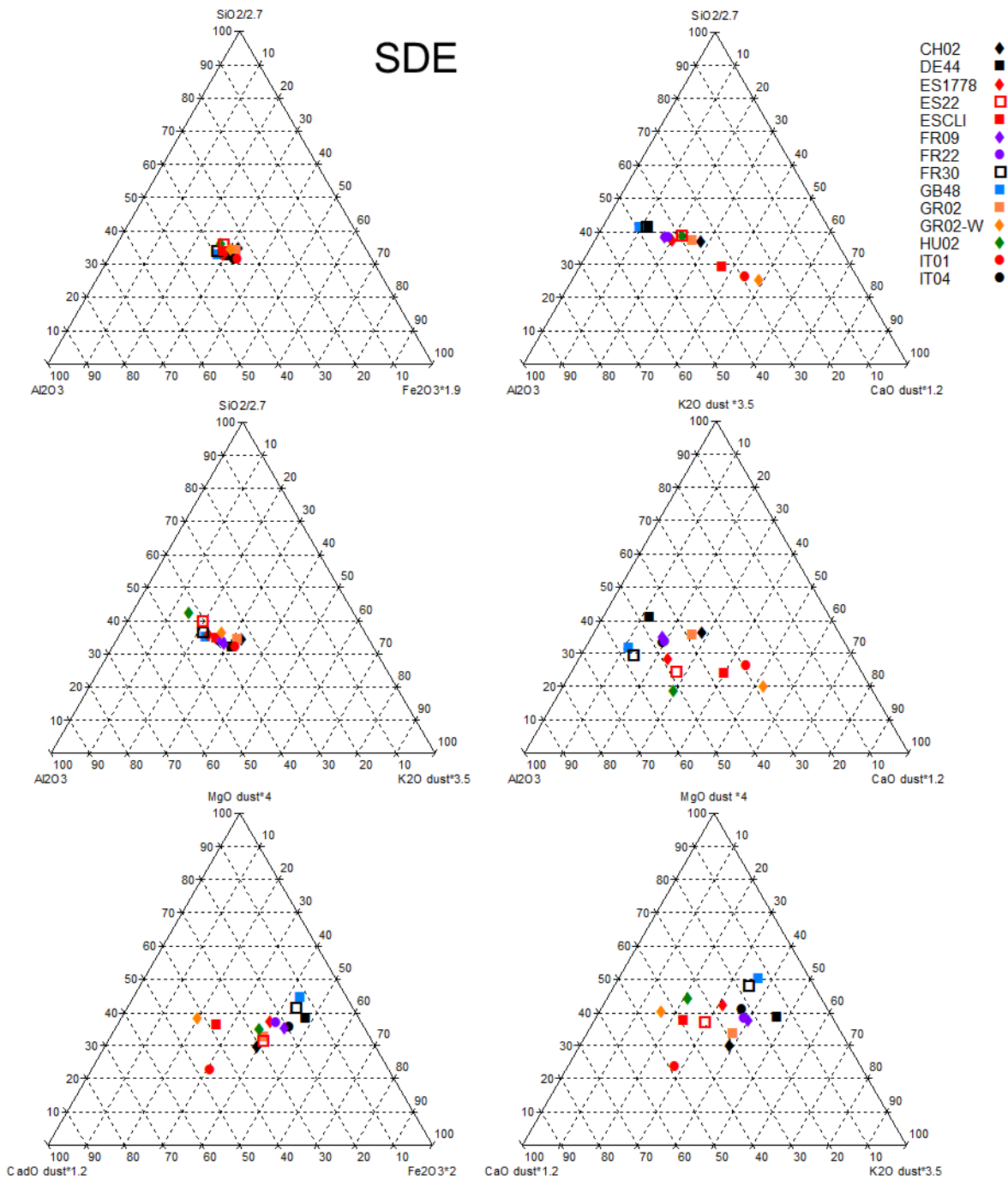
**Figure S5:** Ternary diagrams for major mineral components for days with Saharan dust impact (SDE). Orange: GR02; red: Southwestern and Central Southern Europe sites; purple: Central Western Europe; black: Central Europe sites; blue; Northern Europe and Atlantic sites; green: Eastern Europe sites; empty symbols: high altitude sites.
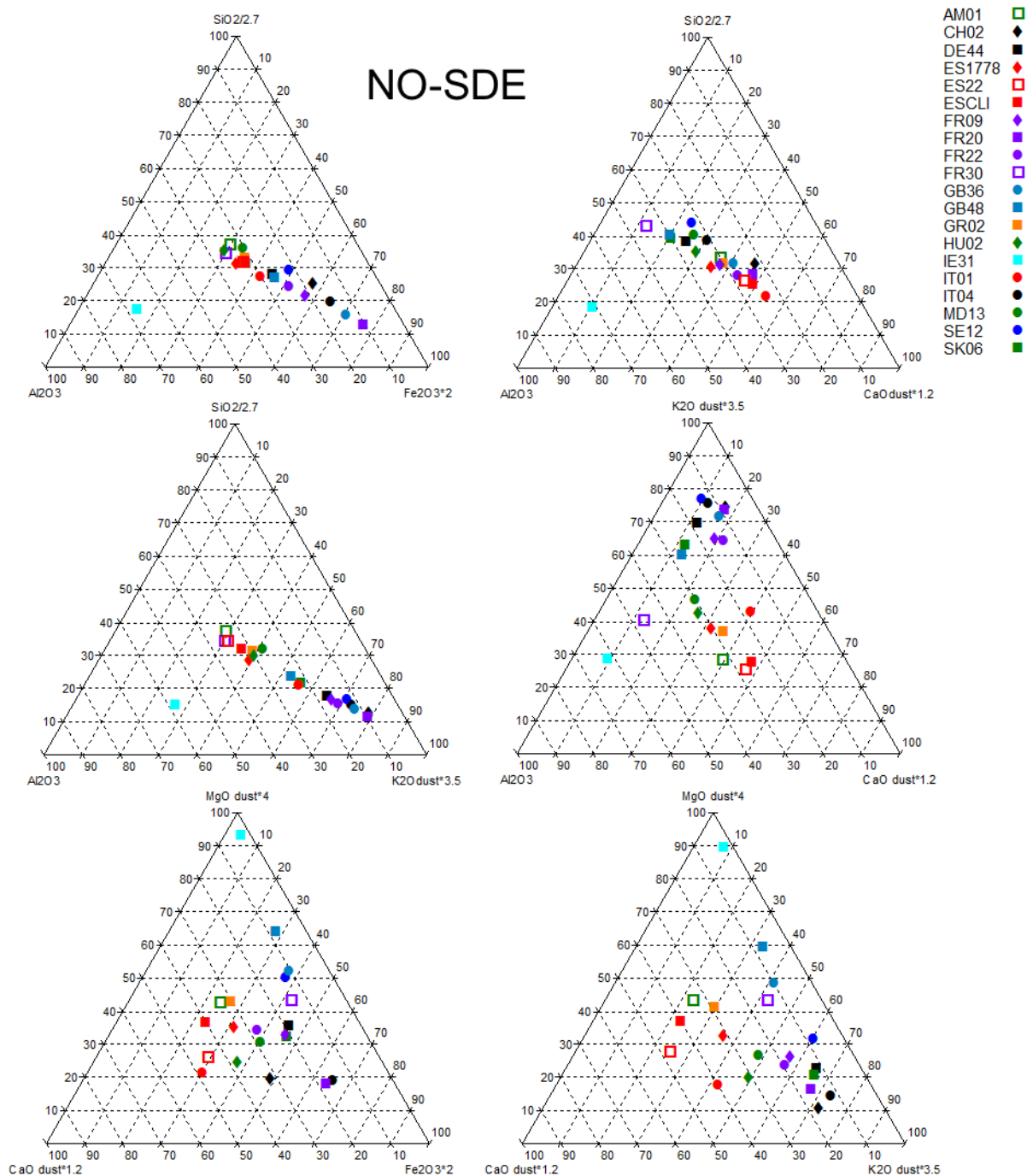
**Figure S6: Ternary diagrams for average concentration (considering the two IMPs) of mineral dust major components for days without impact of Saharan dust (NO-SDE). Orange: GR02; red: Southwestern and Central Southern Europe; purple: Central Western Europe; black: Central Europe; blue; Northern Europe; green: Eastern Europe; empty symbols: high altitude sites.**
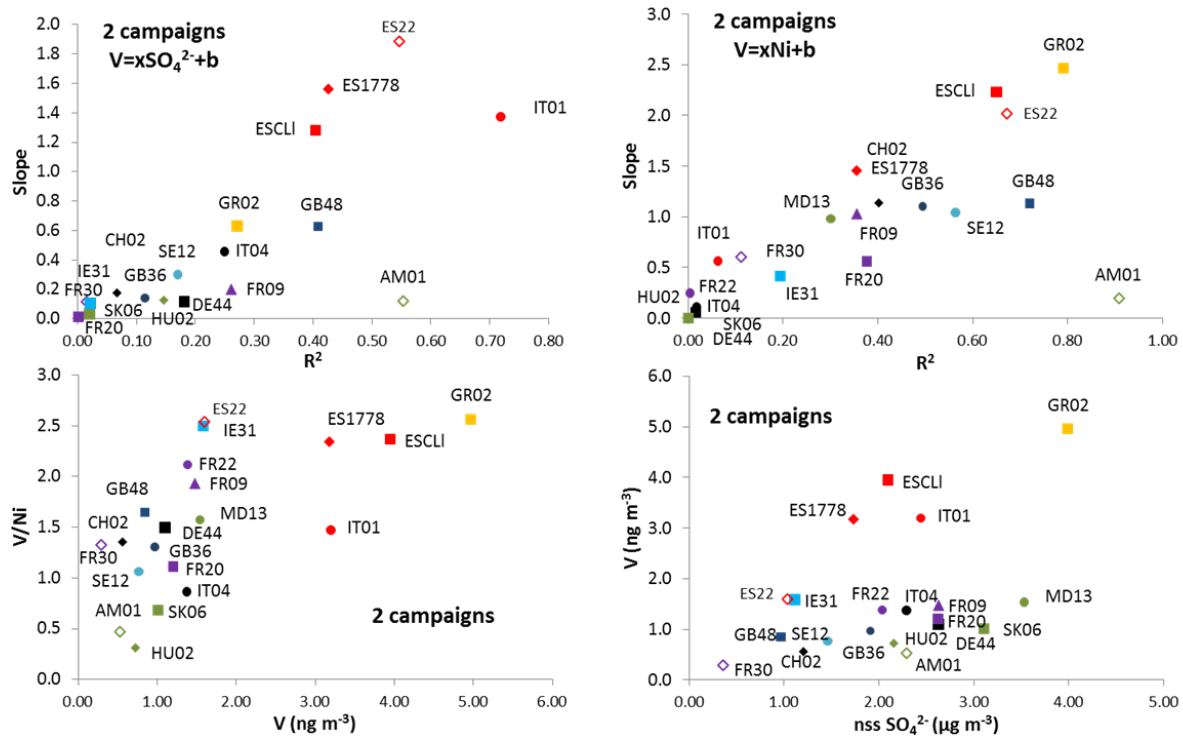
**Figure S7:** Scatter plots for: Top – determination coefficients ($R^2$) and the slopes (x) of the regression equations (V (ng m$^{-3}$) = xSO$_4^{2-}$( μg m$^{-3}$) +b, and V (ng m$^{-3}$)= m Ni (ng m$^{-3}$)) calculated at each site considering the two IMPs; Bottom - the ratio V/Ni with V concentrations and the averaged concentrations of V with SO$_4^{2-}$.
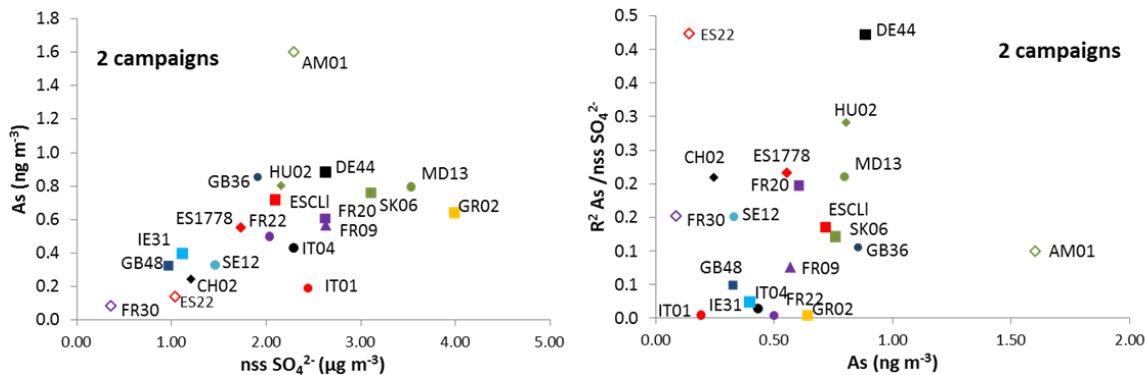
**Figure S8:** Scatter plots for correlation coefficients ($R^2$) and the slopes (x) of the regression equations (As (ng m$^{-3}$)= xSO$_4^{2-}$(µg m$^{-3}$) +b), calculated at each site considering the two IMPs. Correlation of As concentrations with nssSO$_4^{2-}$ and with the $R^2$ coefficients.
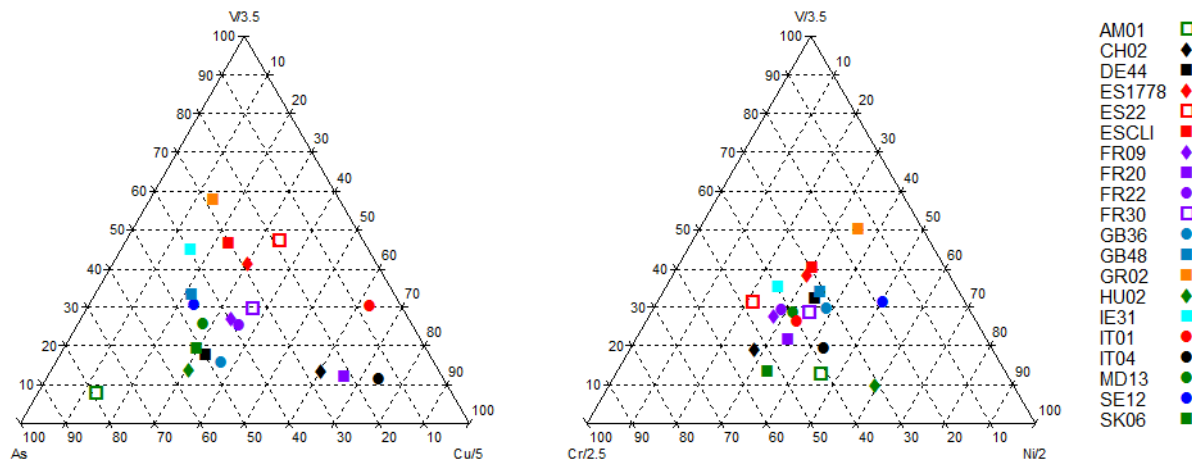


**Figure S9:** Ternary diagrams for traffic (Cu), fuel combustion (V/Ni), coal combustion (As) and industrial (metallurgy, Cr, Ni) trace metal tracers for NO-SDE sampling days during the EMEP IMPs. Orange: GR02; red: Southwestern and Central Southern Europe sites; purple: Central Western Europe; black: Central Europe sites; blue; Northern Europe and Atlantic sites; green: Eastern Europe sites; empty symbols: high altitude sites.